Planta (2017) 246:105–122
DOI 10.1007/s00425-017-2691-y

ORIGINAL ARTICLE

Rice fatty acyl-CoA synthetase OsACOS12 is required for tapetum programmed cell death and male fertility

Xijia Yang[1] · Wanqi Liang[1] · Minjiao Chen[1] · Dabing Zhang[1,2,3] · Xiangxiang Zhao[3] · Jianxin Shi[1,3]

Received: 25 January 2017 / Accepted: 2 April 2017 / Published online: 5 April 2017

Abstract

Main Conclusion **Loss of function mutation of rice OsACOS12 impairs lipid metabolism-mediated anther cuticle and pollen wall formation, and interferes with tapetum programmed cell death, leading to male sterility.**

Acyl-CoA Synthetase (ACOS) is one of the enzymes activating fatty acids for various metabolic functions in plants. Here, we show that OsACOS12, an orthologue of Arabidopsis ACOS5 in rice, is crucial for rice fertility. Similar to *acos5*, *osaocs12* mutant had no mature pollen. But unlike *acos5*, *osaocs12* produced defective anthers lacking cutin and Ubisch bodies on the epidermal and inner surfaces, respectively, and delayed programmed cell death (PCD)-induced tapetum degradation. Those phenotypic changes were evident at stage 10, during which *OsACOS12* had its maximum expression in tapetal cells and microspores. Chemical analysis revealed that the levels of anther cuticular lipid components (wax and cutin monomers) were significantly reduced in *osaocs12*, while the expression levels of three known lipid biosynthetic genes were unchanged. Recombinant OsACOS12 enzyme was shown to catalyze the conversion of C18:1 fatty acid to C18:1 CoA in vitro. Phylogenetic analysis indicated that OsACOS12 is an ancient and conserved enzyme associated with the plant's colonization to earth. Collectively, our study suggests that OsACOS12 is an ancient enzyme participating in a conserved metabolic pathway for diversified biochemical functions to secure male reproduction in plants.

Keywords Acyl-activating enzyme · Anther cuticle · Male sterility · *Oryza sativa* · Pollen exine

Abbreviations

FID	Flame ionization detector
GC–MS	Gas chromatography–mass spectrometry
GUS	β-Glucuronidase
PCD	Programmed cell death
HPLC–MS/MS	High-performance liquid chromatography–mass spectrometer/mass spectrometry
SEM	Scanning electron microscopy
TEM	Transmission electron microscopy
TUNEL	Terminal deoxynucleotidyl transferase-mediated dUTP nick-end labeling

Introduction

Fatty acids play fundamental roles in plant development in general and plant reproductive development in particular (Jiang et al. 2013; Shi et al. 2015). They are indispensable structural components of cellular membrane glycerolipids

Electronic supplementary material The online version of this article (doi:10.1007/s00425-017-2691-y) contains supplementary material, which is available to authorized users.

✉ Jianxin Shi
jianxin.shi@sjtu.edu.cn

[1] Joint International Research Laboratory of Metabolic and Developmental Sciences, Shanghai Jiao Tong University–University of Adelaide Joint Centre for Agriculture and Health, School of Life Sciences and Biotechnology, Shanghai Jiao Tong University, Shanghai 200240, China

[2] Plant Genomics Center, School of Agriculture, Food and Wine, University of Adelaide, Waite Campus, Urrbrae, SA 5064, Australia

[3] Key Laboratory of Crop Marker-Assisted Breeding of Huaian Municipality, Jiangsu Collaborative Innovation Center of Regional Modern Agriculture and Environmental Protection, Huaian 223300, China

and seed storage lipids (such as triacylglycerol) (Li-Beisson et al. 2010), and recent studies have highlighted their additional but essential roles in the development of anther cuticles and pollen sporopollenins (Jung et al. 2006; Li et al. 2006, 2010; Ariizumi and Toriyama 2011; Shi et al. 2015; Ischebeck 2016; Zhang et al. 2016). Fatty acids also act as important regulatory signals of plant development (Weber 2002).

Currently, our understanding of the roles that fatty acids play in plant reproductive development is mainly from studies in two important model species: Arabidopsis and rice. Those studies have been focused particularly on the development of anther and pollen, which is a complicated but important process that results in the release of viable pollens for pollination and fertilization. The development of anther and pollen in both species shares similar stages and machineries (Wilson and Zhang 2009; Shi et al. 2015). When orthologous genes that are involved in fatty acid biosynthesis, modification, transportation, and regulation are mutated in each species, corresponding mutants often display abnormal anther and pollen development with significant reduction or loss of male fertility. Those orthologous genes include *Male Sterility 2* (*MS2*)/*Defective Pollen Wall* (*DPW*) (Chen et al. 2011; Shi et al. 2011), *CYP704B1*/*CYP704B2* (Dobritsa et al. 2009; Li et al. 2010), *CYP703A2*/*CYP703A3* (Morant et al. 2007; Yang et al. 2014), *ABCG26*/*OsABCG15 (PDA1)* (Choi et al. 2011; Zhu et al. 2013; Zhao et al. 2015), and *ABORTED MICROSPORES* (*AMS*)/*Tapetum Degeneration Retardation* (*TDR*) (Xu et al. 2010, 2014; Li et al. 2006). Interestingly, evidence from genetic, molecular, and biochemical analyses indicates that the many of these fatty acid metabolism-related genes are conserved in other plant species as well (Gómez et al. 2015; Shi et al. 2015), highlighting the importance of lipid metabolism in plant reproductive development.

Tapetum is the innermost layer of anther wall. It is a secretory cell layer that functions as the source for synthesis and transport of nutritional and structural molecules (including lipidic compounds such as precursors for pollen exine and tryphine) for pollen wall formation, which undergoes degradation induced by programmed cell death (PCD) during meiosis (Goldberg et al. 1993). Immature or delayed tapetum PCD usually affects pollen development and male sterility in both Arabidopsis and rice (Li et al. 2006; Xu et al. 2010). In rice, increasing evidences have indicated that mutations of certain tapetum-expressed genes including tapetum PCD regulatory genes can lead to defective formation of both anther cuticle and pollen wall (Li et al. 2006, 2010; Li and Zhang 2010; Zhu et al. 2013; Yang et al. 2014; Zhao et al. 2015). These results imply the functional conservation of lipid metabolism-associated genes during reproductive development between dicots (Arabidopsis) and monocots (rice).

In tapetal cells, the de novo biosynthesis of fatty acids occurs in plastids, and the final products are C16 and C18 fatty acids attached with acyl carrier protein (ACP) (Li-Beisson et al. 2010). Those synthesized acyl fatty acid-ACPs have two fates: First, they can be reduced by MS2/DPW to acyl alcohols, which are then allocated out of the plastids (in a yet unknown way) to participate in the formation of anther cuticle and pollen exine (Chen et al. 2011; Shi et al. 2011); Secondly, they can be activated by either long-chain acyl-CoA synthetases (LACS) or acyl-CoA synthetases (ACOS) into fatty acyl CoAs. In the latter case, the activated fatty acyl CoAs can also be exported from the plastids and used in several metabolic pathways (Schnurr et al. 2004; Li-Beisson et al. 2010). Arabidopsis LACS2 has been reported to catalyze the synthesis of ω-hydroxy fatty acyl-CoA intermediates for cutin synthesis in vegetative tissues (Schnurr et al. 2004). Since anther cuticle and pollen wall share common lipid metabolic pathways and regulatory machineries with other plant cuticular lipids (Lallemand et al. 2013; Shi et al. 2015; Wallace et al. 2015), there is increasing interest to reevaluate the roles of LACS and ACOS in plant reproduction. Although single mutant *lacs1* does not show defective phenotype in reproduction, *lacs1lacs2* double mutant displays defective flower development and reduced seed set (Weng et al. 2010). The *acos5* mutant, however, is complete male sterile (de Azevedo Souza et al. 2009), indicating a critical role of ACOS for plant male reproduction.

ACOSs are a large family of phenylpropanoid enzyme 4-coumarate:coenzyme A ligase (4CL)-related enzymes, catalyzing the conversion of free fatty acids to acyl-CoAs in an ATP-dependent manner (de Azevedo Souza et al. 2008). ACOSs are highly conserved in angiosperms and some are land plant specific (Shockey and Browse 2011). Most *ACOS* genes contain peroxisomal target sequences except those in clade V that are single copy in several plant species (de Azevedo Souza et al. 2008, 2009). In clade V, Arabidopsis *ACOS5* is preferentially expressed in flowers (de Azevedo Souza et al. 2008), particularly in tapetum (de Azevedo Souza et al. 2009). Loss of function mutation of *ACOS5* results in male sterility due to defective pollen exine and the absence of mature pollens (de Azevedo Souza et al. 2009). In vitro enzyme activity assay indicates that recombinant ACOS5 is a medium- to long-chain fatty acyl-CoA synthetase that prefers fatty acids with a hydroxyl group at C8–C16 as substrates (de Azevedo Souza et al. 2009). The tobacco orthologue of *ACOS5*, *NtACOS1*, is prominently expressed in tapetum (Varbanova et al. 2003), and RNAi silencing of it leads to defective nexine, as well as significantly reduced pollen number and male sterility (Lin 2012). Similar to *ACOS5* and *NtACOS1*, the ACOS

orthologue in poplar, *PoptrACOS13*, is mainly expressed in male flowers (de Azevedo Souza et al. 2008), although its function has not been characterized yet. *OsACOS12*, the rice orthologue of *ACOS5*, has been reported to be expressed in immature panicles (de Azevedo Souza et al. 2008, 2009), and responsive to low temperature (Yuan et al. 2011). Recently, *OsACOS12* has been reported to be essential for sporopollenin synthesis in *Indica* rice (Li et al. 2016). Although a conserved function of genes in clade V has been proposed (de Aevedo Souza et al. 2009), their exact roles in anther and pollen development have not been established.

In this study, we further characterized *OsACOS12* in rice with focus on its roles in anther and pollen development. The *osacos12* mutant is complete male sterile and its anthers lack spaghetti-like cutin and popcorn-like Ubisch bodies (also called as orbicules) on the outer and inner surfaces, respectively. Notably, the tapetum degradation induced by PCD is delayed in *osacos12,* which results in the failure of exine development. The lacking of anther cutin and pollen exine in *osacos12* is accompanied by concomitant decline of cuticular lipid components in mutant anthers, and the delayed tapetum degradation is coincided with the altered expression patterns of three known tapetum PCD regulatory genes. Further analyses demonstrate that *OsACOS12* is specifically expressed in tapetum and microspores, and it catalyzes the conversion of C18:1 fatty acid to C18:1-CoA in vitro. These results reveal some novel functions of OsACOS12 in male reproductive development that have not been reported for ACOS5.

Materials and methods

Plant materials, growth condition, and phenotypic analysis

All rice plants used in this study were grown in the paddy field of Shanghai Jiao Tong University. The F2 progenies for mapping were generated through a cross between Guangluai 4 (wild type, *indica*) and *osacos12* mutant (*japonica*). Rice plants with male sterile phenotype in F2 populations were chosen for gene mapping.

Phenotypic characterization of the *osacos12* mutant

The phenotypes of the whole plants and their reproductive organs were photographed with a Nikon E995 digital camera. Semi-thin section, scanning electronic microscopy (SEM), terminal deoxynucleotidyl transferase-mediated dUTP nick-end labeling (TUNEL) assay, transmission electronic microscopy (TEM), and DAPI staining of microspores were performed as previously described (Li et al. 2006; Zhang et al. 2010; Zhu et al. 2013). Anthers from different developmental stages were collected based on spikelet length and lemma/palea morphology (Zhang and Wilson 2009; Zhang et al. 2011).

Molecular cloning of *OsACOS12* and complementation of the *osacos12* mutant

For fine mapping of the *OsACOS12* locus, bulked segregated analysis was used and 16 pairs of InDel molecular markers were designed based on the sequence difference between *japonica* and *indica* (http://www.ncbi.nlm.nih.gov/). A 5.1 kb genomic sequence of *OsACOS12* including 3.0 kb upstream sequence, 1.9 kb *OsACOS12* coding sequence and 0.2 kb downstream sequence was amplified from wild-type rice genomic DNA. The cloned genomic fragment *of OsACOS12* was subcloned into the binary vector pCAMBIA1301, which contains a hygromycin resistance gene. Calli induced from young panicles of homozygous *osacos12* mutant plants were used for transformation with *Agrobacterium tumefaciens* (EHA105) carrying either pCAMBIA1301-OsACOS12 plasmid or pCAMIBA1301 plasmid as a control. Transgenic plants were identified by PCR analysis, and over 50 positive transgenic plants were obtained for each construct (Primers used are listed in Supplementary Table S1).

Anther cutin and wax determination

Wild-type and mutant anthers at stage 13 were collected, and their cutin and wax contents were analyzed as previously described (Zhu et al. 2013). Surface areas of rice anther were determined from the microscopy images, assuming a cylindrical body for rice anthers as previously reported (Shi et al. 2011) (Supplementary Figure 4).

Phylogenetic analysis

The full-length amino acid sequence of OsACOS12 and 38 of its closest sequences identified via BLAST search were aligned using Muscle 3.6 (http://www.ebi.ac.uk/Tools/msa/muscle/), and the aligned sequences were used to construct a phylogenetic tree using MEGA 4.0 (http://www.megasoftware.net/index.html). The neighbor-joining method was applied with the following parameters: poisson correction, pairwise deletion, and 1000 bootstrap replicates.

RT-PCR, qRT-PCR, GUS activity analysis, and in situ hybridization

Total RNA was isolated from various rice tissues including anthers at different developmental stages using TRI reagent

as described by the supplier (Sigma-Aldrich). For cDNA synthesis, 1 μg RNA per sample was used for reverse transcription using Primescript1 ® RT reagent Kit with gDNA eraser (Takara). RT-PCR was performed using TaKaRa Ex Taq DNA polymerase. The PCR program was 28 cycles of denaturation for 30 s at 94 °C, annealing for 30 s at 55 °C, and extension for 30 min at 72 °C, followed by a final extension for 5 min. qRT-PCR was performed on a thermocycler (Bio-Rad) using SYBR Premix Ex TaqTM GC (Takara) according to the manufacturer's instructions. The parameters for qRT-PCR were as follows: 95 °C for 3 min, followed by 42 cycles of 95 °C for 10 s, 56 °C for 15 s, and 72 °C for 15 s plus 80 °C for 5 s. *OsACTIN* gene was used as an internal reference control, and a relative quantitation method (Δ cycle threshold) was used to quantify the relative expression levels of target genes. Three biological repeats were used for each PCR assay, and each PCR assay was repeated three times to generate a dataset for statistical analysis and error range determination. Primers used are listed in Supplementary Table S2.

To fuse *OsACOS12* promoter with *GUS* (β-glucuronidase) reporter gene, a 3.02 kb upstream sequence of *OsACOS12* gene was amplified from wild-type rice genomic DNA and cloned into the binary vector *pCAMBIA1301* to construct *pOsACOS12::GUS*. GUS activity analysis was performed as previously reported (Li et al. 2010).

For In situ hybridization, two *OsACOS12* cDNA fragments were mixed for preparing antisense and sense probes, respectively (Tan et al. 2012). Primers used are listed in Supplementary Table S3.

Heterologous expression and enzymatic analysis of *OsACOS12*

The full-length *OsACOS12* cDNA encoding a 555 amino acids was synthesized in vitro using optimized codons for protein expression in *Escherichia coli*. The synthesized cDNA was cloned into the bacterial expression vector pET-28a using restriction endonucleases *Bam*HI and *Hin*dIII. Recombinant OsACOS12 protein was expressed in BL_{21}-DE_3 *E. coli* cells. The expressed His-tagged proteins were purified using a Ni^{2+} column. The eluent was analyzed by 10% SDS-PAGE, and determined using a monoclonal antibody against His-tag (Beyotime).

For enzymatic activity analysis of OsACOS12, the reaction mix contained 20 μg of purified recombinant OsACOS12 protein, 50 μM C18:1 FA, 5 mM ATP, 5 mM MgCl2, 1 mM CoA, 2.5 mM DTT, and 60 mM PBS (pH 7.5). After incubation at 37 °C for 30 min, the reaction mix and a positive control standard solution (0.01 mg C18:1-CoA) were analyzed on an ion trap mass spectrometer operating in negative ESI mode. The full mass scan range was from *m/z* 0 to 1500. Putative molecular ions were further characterized by MS–MS fragmentation patterns to confirm the formation of corresponding fatty acyl-CoA esters.

Results

Isolation and genetic analysis of *osacos12* mutant

In the process of the studies on molecular bases controlling rice male fertility, we isolated a complete male sterile mutant from our rice mutant library obtained by treatment 9522 (*japonica* cultivar. L) with ^{60}Co γ irradiation (Chen et al. 2006). The mutant was named as *osacos12* because there was a 17 bp deletion in the first exon of *OsACOS12* gene in the mutant (See below). The *osacos12* mutant plant appeared normal during the vegetative development (Fig. 1a), and its panicles and floral organs were also similar to those of the wild type (Fig. 1b). However, the anthers of *osacos12* were smaller and paler than those of the wild type, lacking mature pollen grains (Fig. 1c–h), while the morphology of the female organ pistil was normal in the mutant (data not shown). All F_1 progenies from the backcross of *osacos12* with wild type displayed wild-type phenotype, and the F_2 progenies displayed an approximate 3:1 segregation ratio of wild-type (fertile) to mutant (sterile) phenotypes (183:57, $\chi^2 = 0.14$, $p > 0.05$), indicating that *osacos12* is caused by a single recessive gene mutation.

Phenotypic analysis of *osacos12* mutant

To investigate the anther morphological changes between *osacos12* and the wild type, the 14 stages of rice anther development process (Zhang and Wilson 2009) were comparatively examined using transverse sections microscopy. There was no detectable morphological difference between *osacos12* and wild-type at the early stages of anther development till stage 9, and during these early stages, *osacos12* anthers underwent normal meiosis and released normal young microspores (Fig. 2a–f). At stage 10, wild-type microspores became round shaped and vacuolated with dark-stained exine, and tapetum became thinner due to the PCD-induced degradation (Fig. 2g). By contrast, *osacos12* microspores collapsed while the tapetal cells became expanded and vacuolated, persisting without degradation (Fig. 2j). At stage 11, the vacuolated wild-type microspores underwent the first mitosis and the tapetum layer condensed into a thin line (Fig. 2h), while the mutant microspores were degraded into fragments, and the tapetum layer became hypertrophic (Fig. 2k). At stage 13, wild-type anther locule was filled with mature pollen grains (Fig. 2i), while *osacos12* anther locule was shriveled and

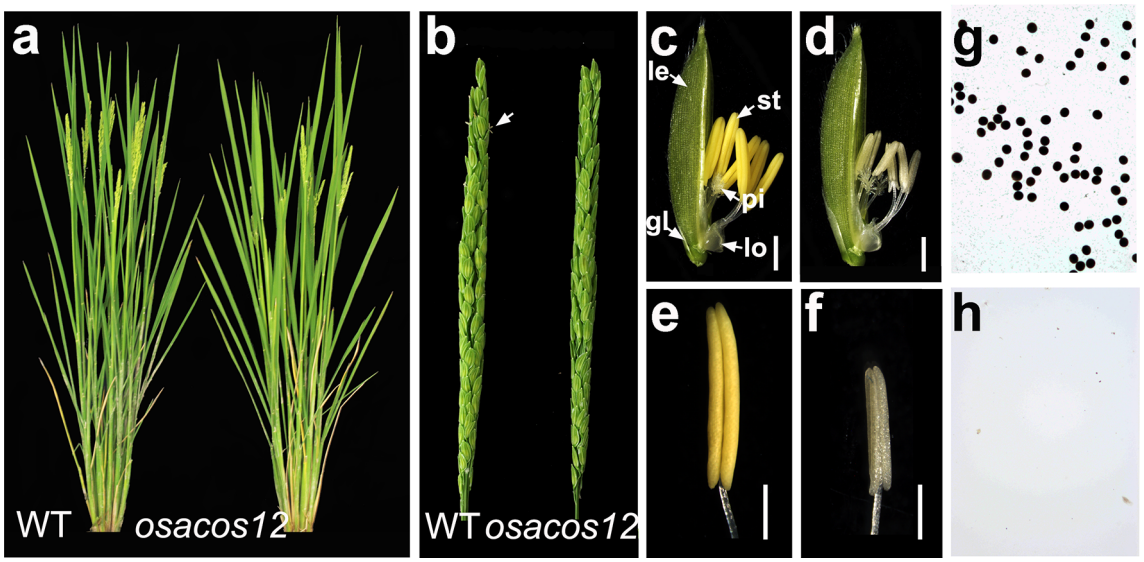

Fig. 1 The phenotype comparison between the wild type and *osacos12* mutant. **a** A wild-type (WT) plant (*left*) and an *osacos12* mutant plant (*right*). **b** A wild-type panicle (*left*) and an *osacos12* mutant panicle (*right*) at the heading stage. The *arrow* indicates anthers. **c** and **d** A wild-type flower (**c**) and an *osacos12* mutant flower (**d**) after removing the palea. *le* Lemma, *gl* glume, *st* stamen, *pi* pistil, *lo* lodicule. **e** and **f** A wild-type anther (**e**) and an *osacos12* mutant anther (**f**). **g** and **h** I_2-KI staining of the pollen grains of the wild-type (**g**) and the *osacos12* mutant (**h**) at stage 13

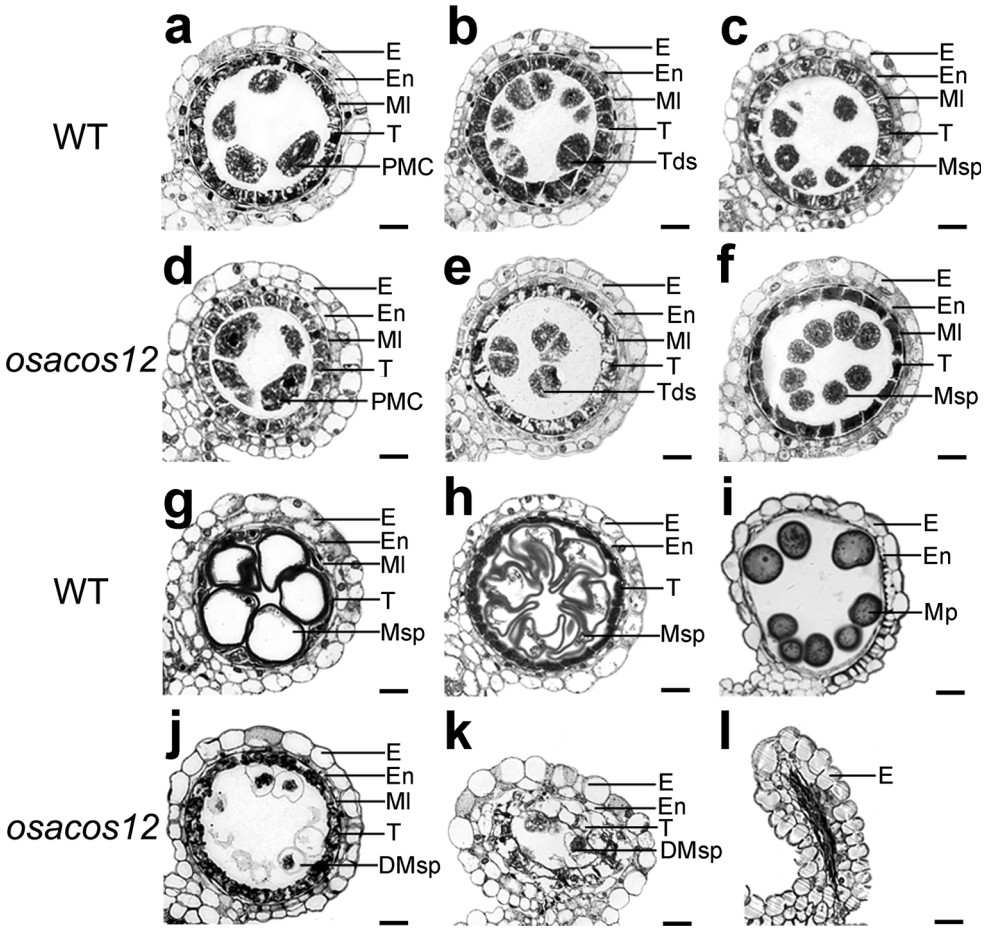

Fig. 2 Analysis of the anther development in the wild type and *osacos12* mutant by transverse section observation. The wild-type anther is shown in **a**–**c**, and **g**–**i**, and the *osacos12* mutant anther is shown in **d**–**f**, and **j**–**l**. Stage 8a [**a** and **d**]; stage 8b [**b** and **e**]; stage 9 [**c** and **f**]; stage 10 [**g** and **j**]; stage 11 [**h** and **k**]; and stage 13 [**i** and **l**]. *DMsp* Degenerated microspores, *E* epidermis, *En* endothecium, *Ml* middle layer, *Mp* mature pollen, *Msp* microspore, *PMC* pollen mother cell, *T* tapetum, *Tds* tetrads

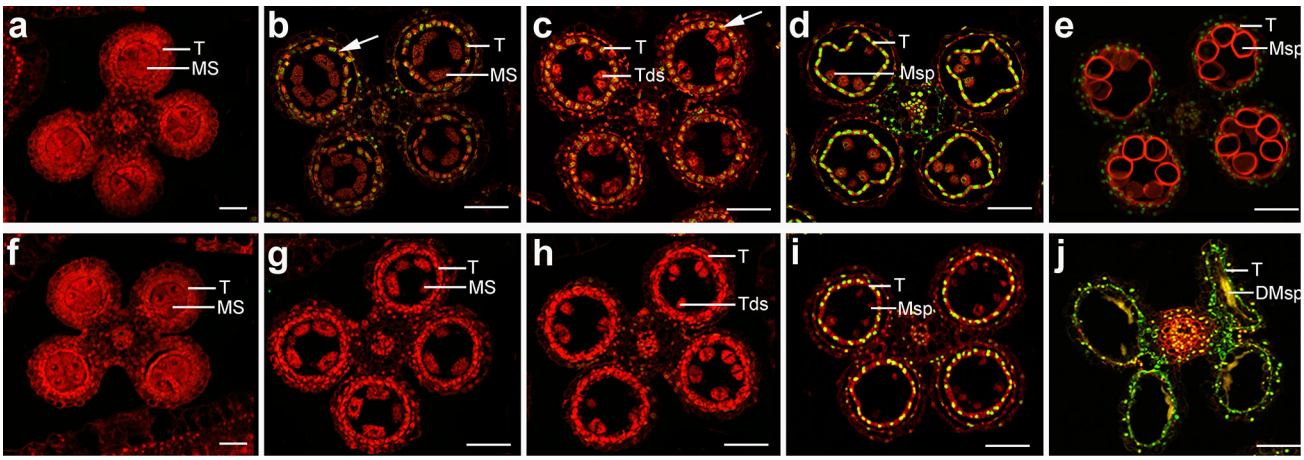

Fig. 3 Detection of DNA fragmentation in wild-type and *osacos12* anthers by TUNEL assay. *Red* signal indicates propidium iodide (PI) staining, *while yellow* and *green fluorescence* indicates TUNEL-positive signal. *DMsp* Degenerated microspore, *Ms* microsporocyte, *Msp* microspore, *T* tapetum. *Bars* = 40 um. **a** and **f** The wild-type and *osacos12* anther at stage 6. **b** and **c** Wild-type anther at stage 8a and stage 8b showing TUNEL-positive signal in tapetal cells (*arrow*). **g** and **h** The *osacos12* mutant anther at stage 8a and stage 8b. **d** and **i** The wild-type and *osacos12* mutant anther at stage 9. TUNEL-positive signal is detected in the tapetum of both wild-type and *osacos12* anthers. Weak TUNEL-positive signal is also observed in the outer cell layers, and vascular bundle cells. **e** The Wild-type anther at stage 10 showing TUNEL-positive signal in the tapetal cells. **j** The *osacos12* mutant at stage 10 showing abnormal distributed TUNEL-positive signal

empty without mature pollen grains (Fig. 2l). These transverse section observations indicated that loss of function mutation of *OsACOS12* severely affects the PCD-induced degradation of tapetum and normal development of pollen in rice.

Delayed PCD of *osacos12* tapetal cells

Since the transverse section observation showed an abnormal tapetal cell degradation in *osacos12*, TUNEL (terminal deoxynucleotidyl transferase-mediated dUTP nick-end labeling) assay was employed to further analyze tapetum PCD process in *osacos12* anthers. TUNEL detects DNA fragmentation based on nicks in the DNA that can be identified by terminal deoxynucleotidyl transferase (TdT), which catalyzes the addition of dUTPs that are secondarily labeled with a marker. At stage 6, when microspore mother cells were generated, there were no obvious PCD signals in both wild-type (Fig. 3a) and *osacos12* (Fig. 3f) tapetal cells. At stage 8a and 8b, positive PCD signals were detected only in the wild-type tapetal cells, suggesting that normal tapetum PCD initiates during the meiosis stage of rice anther development (Fig. 3b, c, g, h). At stage 9, when PCD signals in wild-type tapetal cells became the strongest (Fig. 3d), positive PCD signals were detectable in *osacos12* tapetum (Fig. 3i). At stage 10, PCD signals in the degenerating wild-type tapetal cells became weaker (Fig. 3e), while they continued to increase in *osacos12* anthers (Fig. 3j). These TUNEL assay results suggested that the tapetum PCD in *osacos12* is delayed.

Fig. 4 TEM analysis of anther development in the wild type and *osacos12* mutant. **a**–**d** The wild-type anthers at stage 8b (**a**), stage 9 (**b**), stage 10 (**c**), and stage 13 (**d**). **e**–**h** The *osacos12* anthers at stage 8b (**e**), stage 9 (**f**), stage 10 (**g**), and stage 13 (**h**). **i**–**k** The pollen exine development of the wild type from stage 8b to stage 10. **m**–**o** The pollen exine development of *osacos12* from stage 8b to stage 10. **l** and **p** Ubisch bodies of the wild type (**l**) and *osacos12* (**p**) at stage 10. **q**–**t** The anther epidermis in the wild type at stage 8b (**q**), stage 9 (**r**), stage 10 (**s**), and stage 13 (**t**). **u**–**x** The anther epidermis in *osacos12* at stage 8b (**u**), stage 9 (**v**), stage 10 (**w**), and stage 13 (**x**). *AOr* Abnormal orbicules (Ubisch bodies), *Ba* bacula, *C* cuticle, *CW* cell wall, *DMsp* degenerated microspore, *DPE* degenerated pollen exine, *E* epidermis, *Ex* exine, *Msp* microspores, *Ne* nexine, *Or* orbicules (Ubisch bodies), *PE* prim-exine, *T* tapetal layer, *Tds* tetrads, *Te* tectum. *Bars* = 10 μm in (**a**), (**d**)–(**f**), and (**h**), 5 μm in (**c**), 0.5 μm in (**i**–**x**)

Defective formation of anther cuticle and pollen exine in *osacos12*

For more detailed investigation into the ultramicroscopic changes of anther development in *osacos12*, transmission electron microscopy (TEM) was applied. Consistent with the transverse section results, no obvious ultrastructural difference was observed between wild-type and the *osacos12* mutant anthers before stage 8b (Fig. 4a, e); the primexine formed normally in both (Fig. 4i, m), and their anther cuticle structure looked very similar (Fig. 4q, u). At stage 9, wild-type tapetum started to shrink (Fig. 4b) while *osacos12* tapetum continued to expand (Fig. 4f); the typical two-layer structure of pollen exine formed in both wild type and *osacos12,* while mutant exine was much less stained (Fig. 4j, n); at this stage, no difference in anther

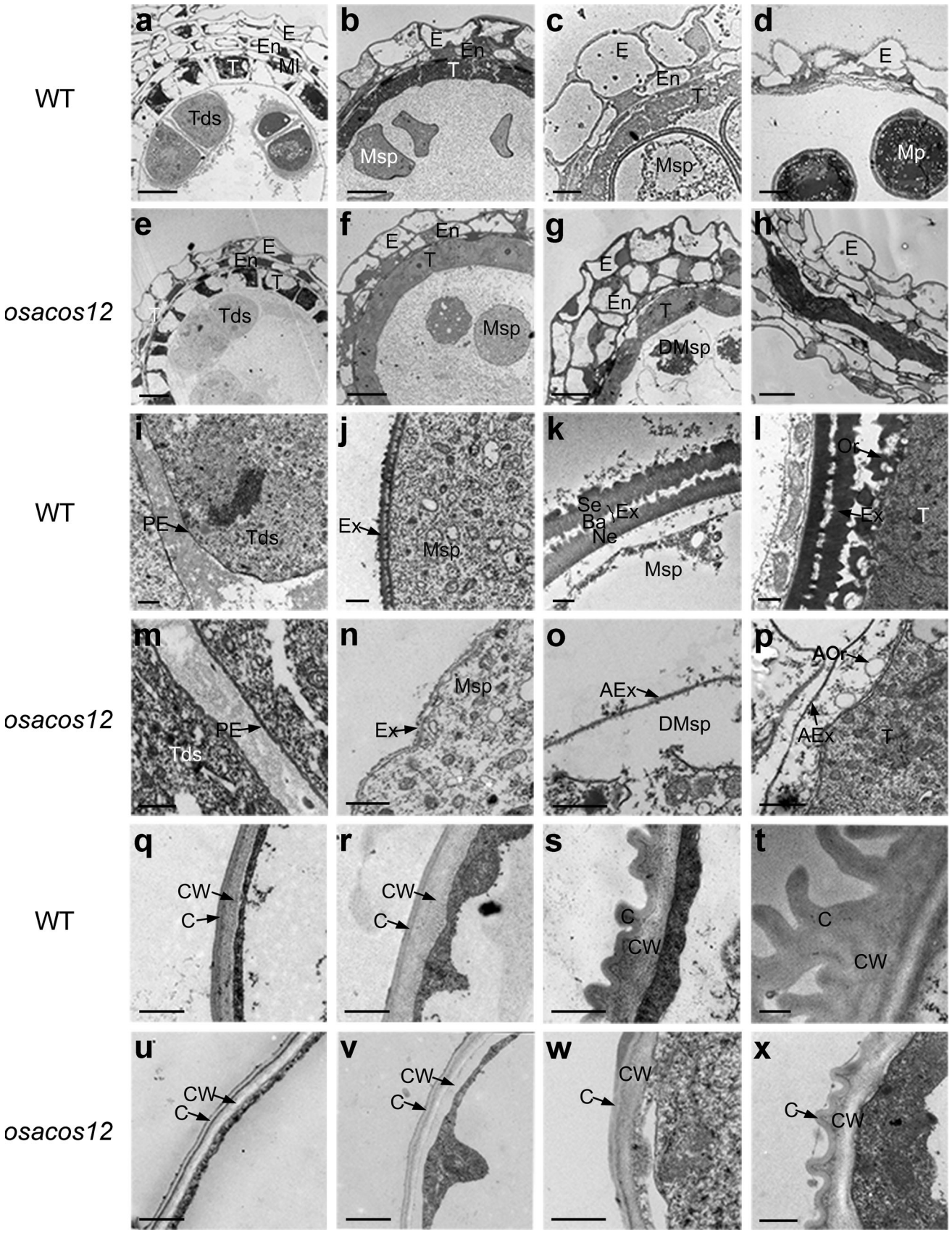
WT
osacos12
WT
osacos12
WT
osacos12
a
E
En
T
Ml
Tds
b
E
En
T
Msp
c
E
En
T
Msp
d
E
Mp
e
E
En
T
T
Tds
f
E
En
T
Msp
g
E
En
T
DMsp
h
E
i
PE
Tds
j
Ex
Msp
k
Se
Ba
Ne
Ex
Msp
l
Or
Ex
T
m
PE
Tds
n
Msp
Ex
o
AEx
DMsp
p
AOr
AEx
T
q
CW
C
r
CW
C
s
C
CW
t
C
CW
u
CW
C
v
CW
C
w
CW
C
x
C
CW

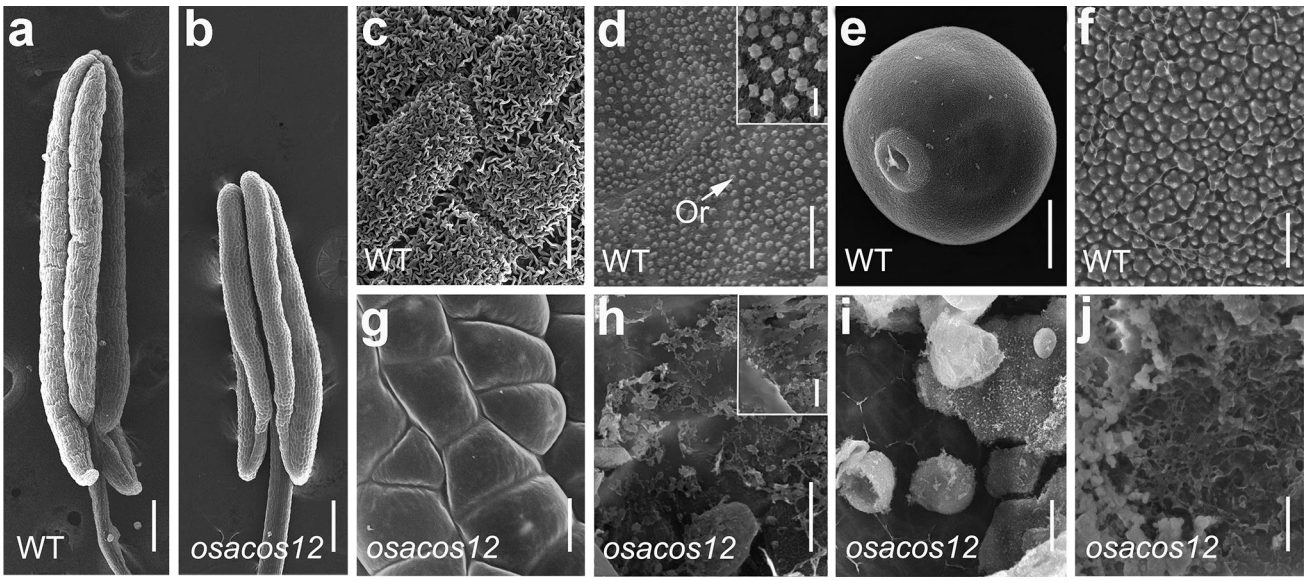

Fig. 5 Scanning electron microscopy analysis of the anthers and pollen grains in the wild type and *osacos12* mutant. **a** and **b** Anthers from the wild type (**a**) and *osacos12* (**b**) at stage 13. **c** and **g** The epidermis of the wild-type (**c**) and *osacos12* (**f**) anthers at stage 13. **d** and **h** The inner surface of the anther wall of the wild type (**d**) and *osacos12* (**g**) at stage 13. The enlarged situation is *boxed*. **e** and **i** The pollen grains of the wild type (**e**) and *osacos12* (**h**) at stage 11. **f** and **j** The enlarged surface on the pollen exine of the wild-type (**f**) and *osacos12* (**i**) at early stage 11. *Bars* = 200 μm in (**a**) and (**b**); 10 μm in (**c**), (**e**), (**f**), and (**h**); 5 μm in (**d**) and (**g**); 1 μm in (**f**), (**i**), and the *boxed* figures

cuticle structure was observed between wild type and *osacos12* (Fig. 4r, v). At stage 10, the wild-type tapetum was degraded into fragments while the mutant tapetum persisted (Fig. 4c, l); the wild-type pollen exine developed normally (Fig. 4k) but *osacos12* pollen exine developed abnormally (Fig. 4o), and the deposition of anther cuticle in *osacos12* also appeared defective at this stage (Fig. 4s, w). At stage 13, the wild-type anther locule was filled with mature pollens while the *osacos12* anther locule was completely empty (Fig. 4d, h); the inner surface of the wild-type anther displayed well-developed Ubisch bodies (Fig. 4l) while the inner surface of *osacos12* anther contained abnormal Ubisch bodies with much less staining (Fig. 4p). The wild-type anther displayed electron-dense hair-like cutin structures that were well organized on the epidermal surface (Fig. 4t) while the *osacos12* anther epidermis displayed defective cutin with much less and short spaghetti structures (Fig. 4x). These TEM results demonstrated that anther cuticle, pollen exine, and tapetum PCD in *osacos12* mutant are all defective as compared to the wild type.

Scanning electron microscopy (SEM) was also used to examine the surfaces of *osacos12* and wild-type anther and pollen grains. At stage 13, the wild-type anther epidermis (Fig. 5a) was covered with three-dimensional spaghetti-like cutin layers (Fig. 5c) and its inner surface was intensively distributed with popcorn-like Ubisch bodies (Fig. 5d). In *osacos12,* its anther epidermis was smooth (Fig. 5b), lacking the typical spaghetti-like cutin (Fig. 5g), and its inner surface was uneven with randomly distributed flocs of Ubisch bodies (Fig. 5h). Because *osacos12* microspores were almost totally degraded after stage 11, the SEM observation on *osacos12* and wild-type microspores was recorded at stage 11. At this stage, the wild-type microspores looked round and smooth (Fig. 5e), and its epidermis was covered with evenly distributed apophysis (Fig. 5f). In contrast, the degrading microspore in *osacos12* was collapsed and looked like cotton wool balls (Fig. 5i), and their epidermal surfaces were covered with randomly distributed cutin materials (Fig. 5j).

Reduced cuticular lipid components in *osacos12* anthers

The abnormal anther cuticle and pollen exine observed by phenotypic observation suggested that *osacos12* anther may be defective in the synthesis of its lipidic precursors. To confirm this, waxes and cutin monomers in both wild-type and *osacos12* anthers were qualitatively and quantitatively measured by gas chromatography–mass spectrometry (GC–MS) and gas chromatography–flame ionization detection (GC–FID) as previously described (Shi et al. 2011). The results indicated that the levels of both wax and cutin monomers were significantly reduced in *osacos12* anthers as compared with those of the wild type (Fig. 6a). The total waxes measured in *osacos12* were 0.076 μg/mm^2, which was less than half of the level in wild type (0.188 μg/mm^2) (Fig. 6a). This reduction in total wax

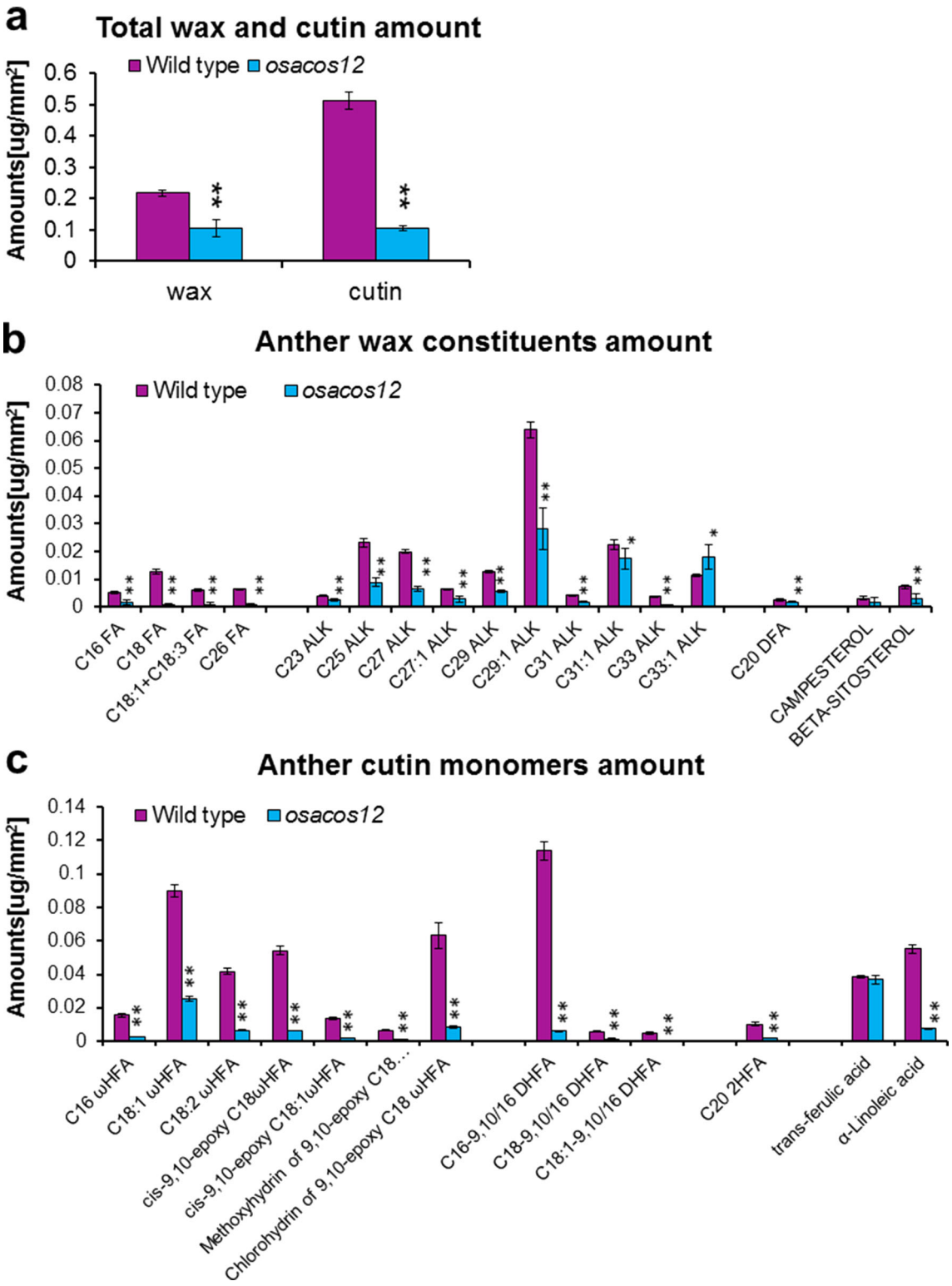

Fig. 6 Chemical analysis of anther cutin and wax in the wild type and *osacos12* mutant. **a** Total cutin and wax amounts per unit surface area (μg cm^{-2}) in wild-type (*blue bars*) and *osacos12* anthers (*red bars*). **b** Cutin monomers amounts per unit surface area (μg cm^{-2}) in wild-type (*blue bars*) and *osacos12* anthers (*red bars*). **c** Wax constituents amounts per unit surface area (μg cm^{-2}) in wild-type (*blue bars*) and *osacos12* anthers (*red bars*). Compound names are abbreviated as follows: *C16 FA* palmitic acid, *C18 FA* stearic acid, *C18:1 FA* oleic acid, *C18:2 FA* linoleic acid, *C18:3 FA* linolenic acids, *C20 FA* arachidic acid, *C22 FA* docosanoic acid, *C26 FA* cerotic acid, *ALK*, alkane

in *osacos12* anthers was contributed largely by the significant reduction of the major rice anther wax components, such as unsaturated alkanes and fatty acids (Fig. 6b; Supplementary Table 4). In addition, the measured anther cutin in *osacos12* was 0.128 μg/mm^2, which was one-sixth of that in wild type (0.721 μg/mm^2) (Fig. 6a). This reduction was contributed mainly to the significant reduction of the dominant rice anther cutin monomers, such as ω-hydroxylated fatty acids and C16-9,10/16 di-hydroxylated fatty acid (Fig. 6c; Supplementary Table 5). These data indicated that the biosynthesis of the lipidic precursors that are required for the formation of anther cuticle and pollen exine is indeed altered in the *OsACOS12* mutant.

Map-based cloning of *OsACOS12*

To identify the mutant gene, a map-based cloning approach was used. Through fine mapping, the target was located to a genetic distance between 23.3 and 24.1 cm on the chromosome 4 (Fig. 7a). In this region, several candidate genes that are putative orthologous of Arabidopsis genes associated with male sterility were selected for sequencing. Among them, *Os04g24530* (*OsACOS12*) had a 17 bp deletion in its first exon, which leads to the shift of the open reading frame. The transcribed *OsACOS12* includes a 194-bp 5′ untranslated region (UTR), a 209-bp 3′ UTR, and a 1668 bp open reading frame (Fig. 7b, c). To confirm that the mutant was caused by the mutation of this gene, complementation of *osacos12* homozygous plants with construct including 3015 bp promoter sequence and the whole genome DNA of *Os04g24530* was carried out, and the fertility of the transformant could be successfully restored (Supplementary Figure 1).

OsACOS12 belongs to an ancient and conserved plant-specific clade of 4 CL-like genes

A previous study has suggested that *OsACOS12* and Arabidopsis *ACOS5* genes are both single-copy genes, and they belong to the same clade, which is a distinct phylogenetic sister group of 4CLs (de Azevedo Souza et al. 2008). To further understand the relationship between *OsACOS12* and its orthologues, the full-length protein sequence of OsACOS12 was used as the query in BlastP to search in three public databases: National Center for Biotechnology Information (NCBI, http://www.ncbi.nlm.nih.gov/), Gramene (http://www.gramene.org/), and The Arabidopsis Information Resource (TAIR, http://www.arabidopsis.org/). A total of 39 orthologous protein sequences from Arabidopsis, rice, *P. patens*, Zea mays, Sorghum bicolor, *Glycine max*, *Mus musculus*, and *Homo sapiens* were selected to construct an unrooted neighbor-joining phylogenetic tree. The tree had clearly four clades (Fig. 8). Clade I is the biggest clade with 20 members from six species including *P. patens*, rice and Arabidopsis, and four of them are the members of Arabidopsis 4CL family. Clade

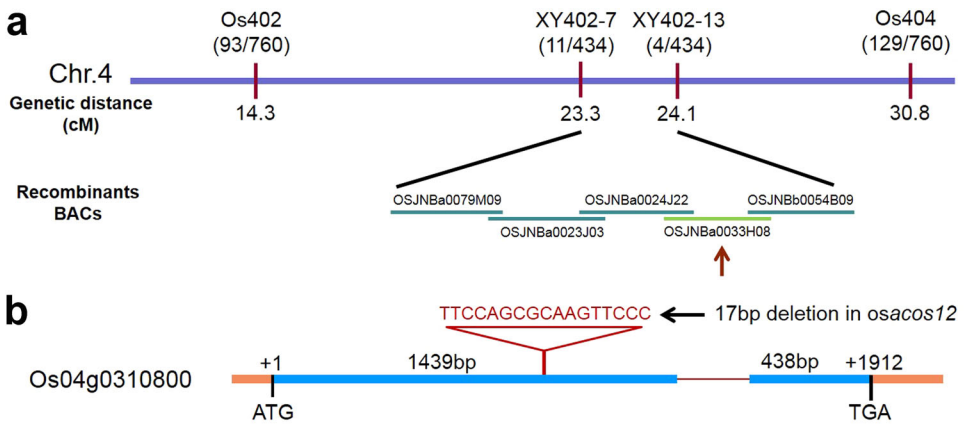

Fig. 7 Map-cloning and sequence analysis of Os*ACOS12*. **a** Fine mapping of the Os*ACOS12* gene on chromosome 4. Names and positions of the molecular markers are indicated. **b** A schematic representation of the exon and intron organization of Os*ACOS12*. The mutant sequence has 17 bases deletion in the first exon. +1 indicates the starting nucleotide of translation (ATG), and the stop codon (TGA) is +1912. *Black boxes* indicate exons, and *intervening lines* indicate introns. **c** The amino acid sequence of OsACOS12. The AMP binding domain is *shaded*. The *red triangle* shows the position of base deletion

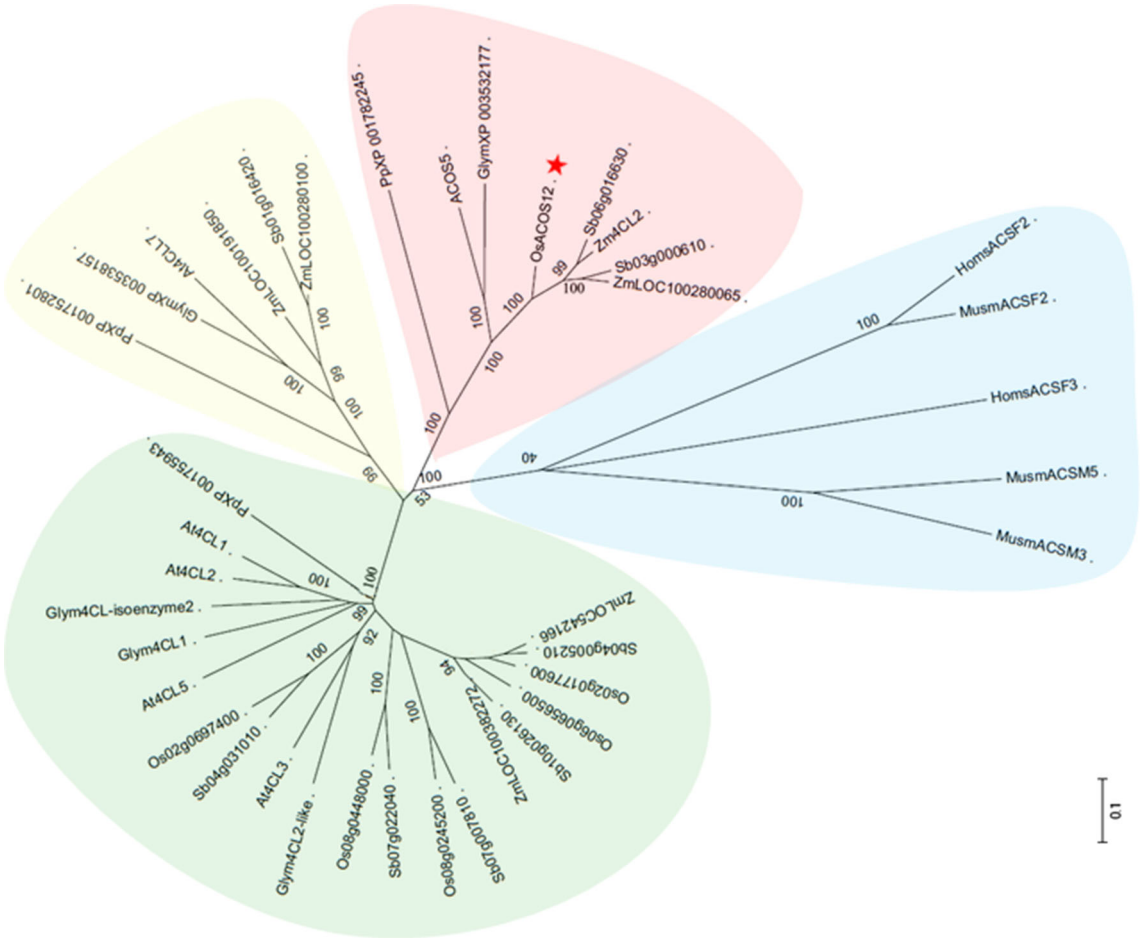

Fig. 8 An unrooted Neighbor-Joining phylogenetic tree of evolutionary relationships among the OsACOS12 and related proteins. A neighbor-joining phylogenetic tree was constructed using MEGA 4.0 to summarize the evolutionary relationships among the OsACOS12 and related proteins. Bootstrap values are percentage of 1000 replicates. At *Arabidopsis thaliana*, Glym *Glycine max*, Homs *Homo sapiens*, Musm *Mus musculus*, Os *Oryza sativa,* Pp *Physcomitrella patens,* Sb *Sorghum bicolor*, Ta *Triticum aestivum*, Zm *Zea mays*

II contains six members from Arabidopsis, *P. patens*, maize, sorghum, and soybean. Clade III includes OsACOS12, ACOS5, and six other members from *P. patens*, maize, sorghum, and soybean. Clade V has five members from animals, such as HomsACSF2 (Acyl-CoA synthetase family), HomsACSF3, MusmACSF2, MusmACSM5 (Acyl-CoA synthetase medium-chain family), and MusmACSM3. In addition, Clade I to Clade III all have members from *P. patens*, a moss. This phylogenetic analysis thus suggested that OsACOS12 is an ancient and conserved enzyme that functions both in water and land plants.

OsACOS12 is mainly expressed in tapetum and microspores

While the vegetative growth of *osacos12* mutant was normal, the main defects happened in the reproductive stages, especially during anther development. The expression pattern of *OsACOS12* was examined by semi-quantitative RT-PCR and quantitative RT-PCR (qRT-PCR) analyses using total RNA extracted from both vegetative and reproductive organs as templates. The results indicated that the expression of *OsACOS12* was not detectable in vegetative tissues such as roots, shoots, and leaves. In reproductive tissues, the expression of *OsACOS12* was very weak in palea/lemma, but very strong in anthers. The expression started at stage 8b, peaked at stage 10, then dropped rapidly to a relative low level at stage 11, and finally became undetectable at stage 12 (Fig. 9a, b). The anther preferable expression pattern of *OsACOS12* was further confirmed by GUS staining assay using transgenic rice plants expressing OsACOS12pro:GUS fusion protein. GUS signals became detectable in anthers at stage 9, peaked at stage 10, declined quickly at stage 11, and became undetectable at stage 12 (Fig. 9c). To determine the spatial and temporal profile of *OsACOS12* expression more precisely, RNA in situ hybridization in wild-type

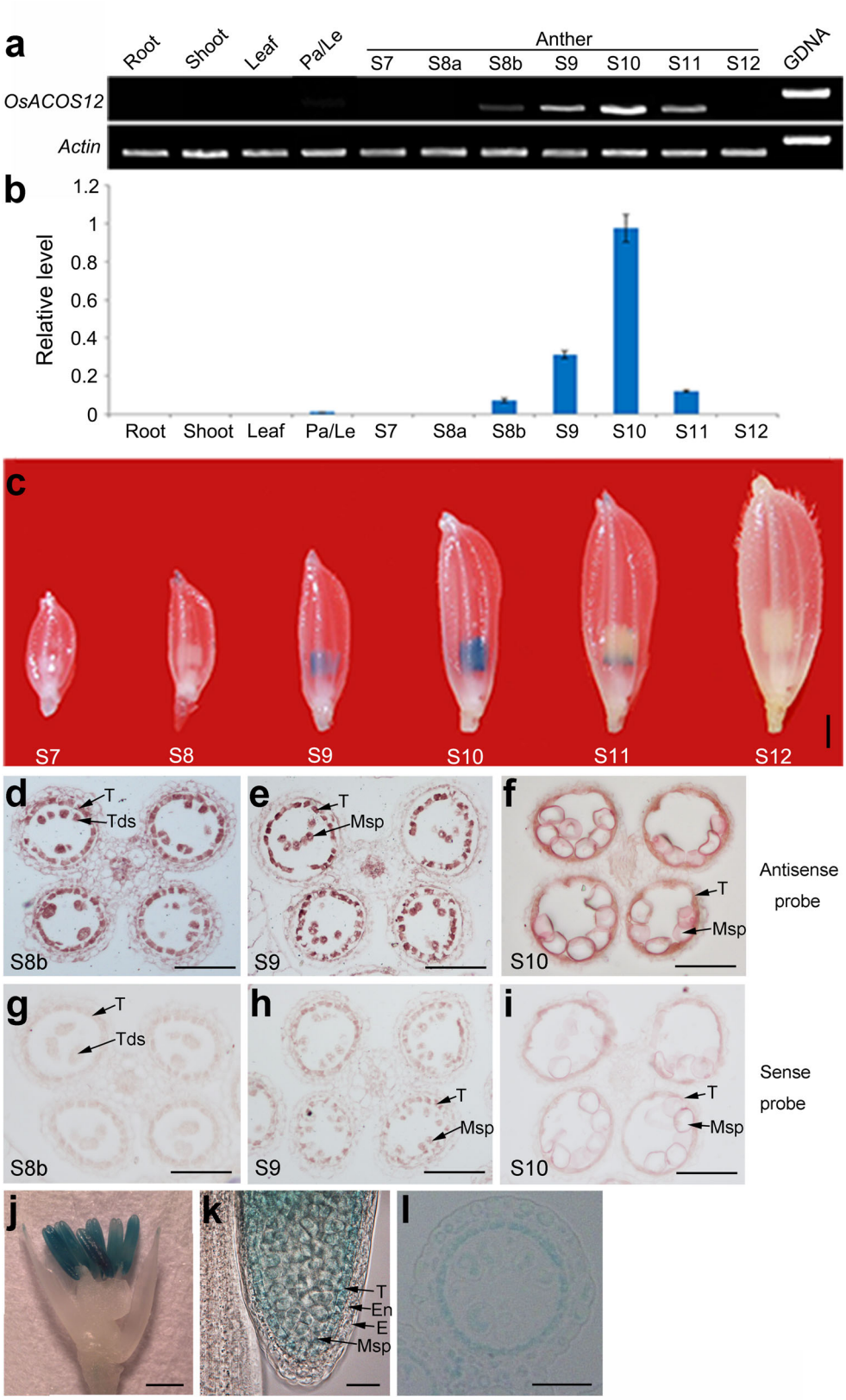

Fig. 9 Expression pattern of *OsACOS12*. **a** Spatial and temporal expression analysis of *OsACOS12* by semi-quantitative RT-PCR. Actin1 serves as a control. **b** qRT-PCR analysis of *OsACOS12*. Data are presented as Mean ± SD ($n = 3$). **c** GUS activity analysis in the anthers of pOsACOS12::GUS transgenic lines at various developmental stages. **d–f** In situ hybridization analysis of *OsACOS12* in wild-type anthers. The anthers at stage 8b (**d**), stage 9 (**e**), and stage 10 (**f**) showing strong signals of *OsACOS12* in tapetal cells and microspores. **g–i** The anthers at stage 8b (**g**), stage 9 (**h**), and stage 10 (**i**) hybridized with *OsACOS12* sense probe. **j** GUS staining in the flower at early stage 10 after removing the palea and lemma. **k** A flattened anther at early stage 10 with GUS staining. **l** Transverse section of the GUS stained anther at early stage 10. *Le* Lemma, *Pa* palea. *S7* stage 7, *S8a* stage 8a, *S8b* stage 8b, *S9* stage 9, *S10* stage 10, *S11* stage 11, *S12* stage 12. *Bar* = 1 mm in (**c**), 50 μm in (**d**)–(**i**), 1.2 mm in (**j**), 10 μm in (**k**), 25 μm in (**l**)

Table 1 Molecular masses of CoA-ester products formed in vitro from oleic acid (C18:1) by OsACOS12

Molecular sources	Molecular species	Mass (calc.)	Enzyme reaction mass (obs.)	C18:1-CoA standard mass (obs.)
Substrates	Fatty acid	282.26		
Products	Fatty acyl-CoA	1031.36		
MS spectrum	$[M–H]^-$	1030.35	1030.35	1030.35
	$[M–H]2^-$	514.67	514.67	514.66
MS–MS spectrum	$[M–H_2O–H]^-$	1012.34	ND	ND
	$[M–2H_2O–H]^-$	994.33	ND	ND
	$[M–HPO_3–H]^-$	950.39	950.39	950.39
	$[M–H_3PO_4–H]^-$	932.38	ND	ND
	$[M–AMP–H]^-$	701.3	ND	ND
	$[M–AMP–H_2O–H]^-$	683.29	683.29	683.29
	$[M–ADP–H]^-$	621.33	ND	ND
	$[ADP–H]^-$	426.02	ND	ND
	$[ADP–H_2O–H]^-$	408.01	408.00	408.01
	$[AMP–H]^-$	346.06	ND	ND

For product analysis, the reaction mix contained 20 μg of purified recombinant OsACOS12 protein, 50 μM C18:1 FA, 5 mM ATP, 5 mM MgCl2, 1 mM CoA, 2.5 mM DTT, and 60 mM PBS (pH 7.5). After an incubation period of 30 min at 37 °C, the reaction samples and the standard sample (0.01 mg C18:1-CoA) as the positive control were infused via nano ESI source into an ion trap mass spectrometer operating in negative ion mode. Mass spectra were obtained by scanning from *m/z* 0 to 1500. Putative product peaks were further characterized by MS–MS analysis resulting in fragments, thereby confirming formation of the corresponding fatty acyl-CoA esters

floral sections was performed, and positive signals were detected in microspores and tapetum in anthers from stage 8b to stage 10 (Fig. 9d, f), showing enhanced expression of *OsACOS12* in these stages. The in situ hybridization results were consistent with the results of light microscopy observations, in which GUS signals were only observed in tapetum and microspores (Fig. 9k, l). The tapetum– and microspore-specific expression of *OsACOS12* implied important functions of OsACOS12 in rice anther development.

Biochemical function of OsACOS12

Arabidopsis ACOS5 has a wide substrate selectivity, and it preferentially catalyzes medium- and long-chain fatty acids represented by oleic acid (C18:1). To test whether OsACOS12 has similar biochemical function as that of ACOS5, recombinant OsACOS12 protein was expressed in *Escherichia coli* BL21 (DE3) transformed with a protein expression construct containing a modified full-length OsACOS12 cDNA in the bacterial expression vector pET28a. The expressed protein was purified and used for subsequent biochemical analysis using oleic acid as a candidate substrate. The in vitro reaction mixture contained the purified recombinant OsACOS12 protein, oleic acid, CoA, and DTT. When the reaction was finished, the product was analyzed by HPLC–MS/MS (high-performance liquid chromatography–mass spectrometer/mass spectrometer) with C18:1-CoA chemical standard as the positive control. The results showed that the recombinant OsACOS12 protein generated a product by with the same ionic characteristics as the positive control, confirming the synthesis of C18:1-CoA from oleic acid and CoA in the reaction (Table 1; Supplementary Figure 2). The in vitro analysis of OsACOS12 enzyme activity suggested that OsACOS12 may also be able to catalyze the conversion of C18:1 fatty acid to C18:1-CoA, and the synthesized C18:1-CoA would participates in the subsequent synthesis of cutin, wax, as well as sporopollenin precursors during anther development.

Gene networks of *OsACOS12*

Because the mutation of *OsACOS12* affects a broad range of anther developmental events, such as tapetum PCD, anther cuticle, and pollen exine development, it is plausible to speculate that *OsACOS12* is one component of the conserved gene network that is critical for anther development in rice. Therefore, we examined expression of certain known rice genes involved in tapetum PCD, anther cuticle, and pollen exine formation in both wild type and *osacos12* by qRT-PCR. The expression patterns of three tapetum PCD regulatory genes, TDR (Li et al. 2006), EAT1 (Niu et al. 2013), and OsAPI5 (Li et al. 2011), was first examined in stage 8–10 anthers, and the results showed that the expression of these tapetum PCD regulatory genes in *osacos12* increased steadily along anther development, which differed from their expression patterns in wild-type anthers (Fig. 10a–c). The expression of several biosynthetic genes associated with rice anther cuticle

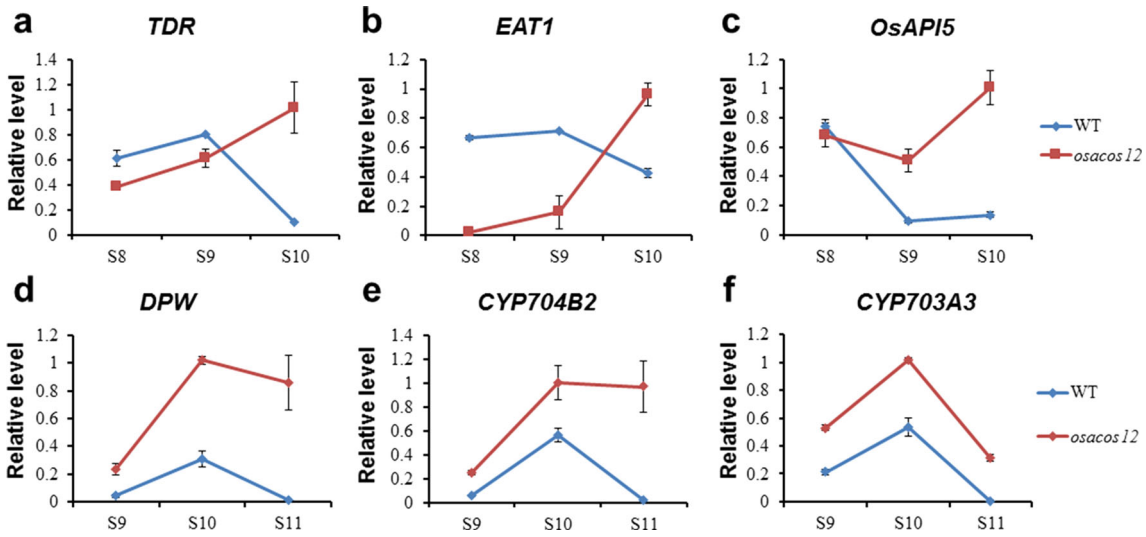

Fig. 10 Expression profile of genes involved in tapetum PCD and lipid metabolism in *osacos12* mutant. Expression analysis of *TDR* (**a**), *EAT1* (**b**), *OsAPI5* (**c**), *DPW* (**d**), *CYP704B2* (**e**), and *CYP703A3* (**f**) in stages 8–10 anthers from the wild type (WT) and the *osacos12* mutant using qRT-PCR. Data are presented as Mean ± SD ($n = 3$). Actin1 serves as a control. *S8* Stage 8, *S9* stage 9, *S10* stage 10, *S11* stage 11

and pollen exine precursors, including *DPW, CYP704B2*, and *CYP703A3*, was also examined. The results showed that the mutation of *OsACOS12* significantly increased the expression of these genes at all tested developmental stages (Fig. 10d–f), reflecting a feedback regulation of lipid metabolism in rice anther and pollen development. Since OsACOS12 mutation had such a broad effects on so many important genes, it is plausible to place it as an important component of the conserved gene regulation network that regulates rice anther and pollen development.

Discussion

Plant male sterility is associated with many abnormal developmental events such as disrupted PCD-induced tapetum degradation (Li et al. 2006; Xu et al. 2010) and altered metabolic activities such as lipid or phenolic metabolism in reproductive organs (Jiang et al. 2013; Lallemand et al. 2013; Shi et al. 2015; Zhao et al. 2015). In this study, we used forward genetics approach combined with biochemical and molecular analyses to characterize the roles of rice *OsACOS12* gene in male fertility and late pollen development. *OsACOS12* encodes a clade III acyl-CoA synthetase (de Azevedo Souza et al. 2008) protein, which can catalyze the conversion of C18:1 fatty acid to C18:1 CoA in vitro, and the mutation of this gene causes abnormal male reproduction in rice. Elucidation of the genetic, molecular, and biochemical mechanisms underlying the functions of *OsACOS12* in male fertility would be important for both basic and practical rice researches.

OsACOS12 is an acyl-CoA synthetase that activates acyl fatty acids with CoA for the formation of anther cuticle and pollen exine in rice

Plant lipids are de novo synthesized in plastids exported out of plastids in the form of CoA conjugates for their diverse biochemical functions. LACS, 4CL, and ACS/ACOS are important acyl-activating enzymes (AAE) involved in this process (Shockey and Browse 2011). LACS participates in both biosynthesis of cutin/suberin and degradation of storage lipids, and 4CL is involved in lignification or biosynthesis of flavonoids. ACOS has several distinct functions in plants (de Azevedo Souza et al. 2008, 2009). In Arabidopsis, the loss of function mutation of ACOS5 causes complete male sterility. The *acos5* mutant does not have mature pollens and fails to produce self-fertilized seeds (de Azevedo Souza et al. 2009). ACOS5 protein is localized in cytoplasm, and *ACOS5* mRNA accumulates in tapetal cells at the early stages of pollen development when the defective phenotype is evident. Because recombinant ACOS5 enzyme preferably takes the medium-chain fatty acids for activation with CoA, and ACOS5 is an ancient acyl-CoA synthetase conserved in land plants (de Azevedo Souza et al. 2009), this report provides evidence for the first time that ACOS functions in a conserved and ancient metabolic pathway that is essential for pollen development in plants. The ACOS gene in tobacco, *NtACOS1*, is also functional in male fertility and pollen exine formation, confirmed by RNAi approach and in vitro enzyme activity assay (Wang et al. 2013). Silencing of *NtACOS1* causes reduced pollen formation and leads to the failure of seed development and

eventually sterility. The mature pollens in NtACOS1 RNAi lines collapse irregularly, Ubisch bodies look hollow, and the exine is defective with abnormal nexine (Wang et al. 2013). Combining with our study and another study in *Indica* rice (Li et al. 2016), these results indicated that ACOS is indeed required for plant male fertility.

Similar to ACOS5 AND nTacos1, the rice OsACOS12 gene also has conserved function in pollen exine formation. While the two-layered pollen exine was still observable in *osacos12* at stage 9 (Fig. 4n), it was severely compromised at stage 10 and 11 when *osacos12* pollen grains collapsed (Fig. 4o, p). In a recent study of OsACOS12 in *Indica* rice, pollen exine was totally absent in collapsed pollen grains at stage 10 (Li et al. 2016). Therefore, the activation of fatty acid with CoA via OsACOS12 is essential for pollen exine formation in rice. Other studies have demonstrated that a series of enzymes, including ACOS, PKSA/B (POLYKETIDE SYNTHASE A/B), and TKPR1/2 (TETRAKETIDE α-PYRONE REDUCTASE1/2), function sequentially along the same biochemical pathway to produce reduced tetraketide α-pyrone for pollen exine formation in Arabidopsis, tobacco, and rapeseed (Grienenberger et al. 2010; Lallemand et al. 2013; Wang et al. 2013; Qin et al. 2016). Although we did not measure tetraketide α-pyrone and the expression of the two downstream genes PKSA/B and TKPR1/2 in *osacos12* in this study, it is clear from available data that fatty acyl CoA precursors generated by OsACOS12 is required for pollen exine formation in rice, and this function of ACOS gene is conserved at least in Arabidopsis, tobacco, rapeseed, and rice.

Besides its conserved function in pollen exine formation, OsACOS12 displays more biological functions than ACOS5 and NtACOS1. The loss of function mutation of *OsACOS12* not only causes defective pollen exine (Fig. 4o, p), but also results in abnormal development of cutin layer (Fig. 4w, x) and Ubisch bodies (Fig. 4p). The effect of OsACOS12 mutation on pollen exine formation has also been reported in another study in *Indica* rice (Li et al. 2016). Since pollen exine and anther cuticle are two important lipidic protective layers of microspores, the involvement of *OsACOS12* in the biosynthesis of both layers indicated a crucial role of *OsACOS12* in male reproductive development. This binary function of *OsACOS12* corresponded well with its specific expression in tapetum and microspore (Fig. 9), and with the specific localization of OsACOS12 protein to the tapetum and anther locule (Li et al. 2016). This result supports previous findings that rice anther cuticle and pollen exine share common lipidic components and that rice genes associated with lipid metabolism has developed both conserved and diverged functions from their Arabidopsis orthologues (Li et al. 2010; Li and Zhang 2010; Fernández Gómez et al. 2015; Shi et al. 2015). The results also imply that the *OsACOS12*-mediated upstream lipid biosynthetic pathway is required by both pollen exine and anther cuticle formation. The mutation of *OsACOS12* affects not only anther wax but also anther cutin in osacos12 mutant, which was not reported in Li's recent study in *Indica* rice (Li et al. 2016).

Nevertheless, the functional network of OsACOS12 in rice anther and pollen development remains unclear; the only report is that the expression of *OsACOS12* along the pollen development is significantly reduced in *gamyb-4* mutant (Supplementary Figure 3). Future investigations need to be focused on in silico analysis of the expression of *OsACOS12* in mutants of known PCD or lipid metabolism-associated transcription factors, as well as identifying potential upstream genetic regulators using genetic and molecular approaches. Interestingly, *OsACOS12*-mediated lipid biosynthesis pathway seems to be regulated by a feedback regulation mechanism, which is evidenced by the enhanced expressions of *DPW*, *CYP704B2*, and *CYP703A3* genes that are known to be associated with anther cuticle and pollen exine (Fig. 10). DPW is an acyl fatty acid reductase converting de novo synthesized fatty acids to fatty alcohols for effective diffusion out of plastids (Shi et al. 2011), and it is a complementary mechanism to OsACOS12-mediated export of fatty acids from plastids. When OsACOS12 is mutated, the expressions of *DPW* in *osacos12* mutant are enhanced. The expressions of *CYP704B2* and *CYP703A3*, two genes encoding in chain hydroxylase, are also increased in osacos12 mutant, likely due to the feedback regulation of lipid metabolism to compensate for the lost function of *OsACOS12*. These findings, together with the reduction of all detected ω-hydroxyl fatty acids, indicate that the preferred substrates of OsACOS12 are fatty acids, which is not as broad as those of ACOS5 and NtACOS1.

OsACOS12 is an important component of tapetum PCD process that is required for timely tapetal cell degradation

It is well known that interference of tapetum PCD process can result in male sterility in plants, because PCD-induced degradation of tapetum is essential for pollen development. This process is tightly regulated, and can be affected by both internal and external factors (Parish and Li 2010). Therefore, Tapetum degeneration provides a useful model system for investigation of molecular mechanisms responsible for plant PCD. Previous studies on Arabidopsis *ACOS5* revealed that although *acos5* mutant displays abnormal pollen wall formation and aborted pollen grain development, there is no observable abnormality of tapetum, and the expression of *ACOS5* is prior to the initiation of tapetum degeneration. Thus, *ACOS5* affects pollen

development via a metabolic pathway without affecting tapetum development and function (de Azevedo Souza et al. 2009). Similarly, tapetum changes were not reported in tobacco *NtACOS1 RNAi* mutant (Lin 2012; Wang et al. 2013) and the *Indica* rice either (Li et al. 2016).

In contrast, the mutation of *OsACOS12* in our study causes aberrant tapetum development. The PCD-induced tapetum degradation is notably delayed in *osacos12* mutant anthers, as TEM and TUNEL assays clearly show late appearance of tapetel cell shrinkage and DNA fragmentation (Figs. 2, 3). The analyses of the expression patterns of *OsACOS12* by in situ hybridization, GUS staining, and qRT-PCR also provide evidence for the involvement of *OsAOCS12* in tapetum development (Fig. 9). The analysis of the expression patterns of three known tapetum PCD regulators (TDR, EAT1, and OsAPI5) in *osacos12* mutant further demonstrates that mutation of *OsACOS12*-disrupted tapetum PCD. Therefore, not only does *OsACOS12* affect tapetum and microspore-specific metabolic pathways that are associated with pollen exine and anther cuticle formation, but also interfere development of tapetum, which is distinct from *ACOS5* and *NtACOS1*. Because *OsACOS12* is sensitive to low temperature (Yuan et al. 2011) in a developmental stage-dependent manner, and tapetum development is most sensitive to abiotic stress (Parish et al. 2012), further elucidation of *OsACOS12* functions and underlying mechanisms for its roles in male fertility would help to reduce crop yield loss, and help breeders to obtain new male sterile varieties for hybrid seed production.

The evolution of OsACOS12 and its conserved function

A previous phylogenetic study on adenylate-forming proteins in Arabidopsis, poplar, and rice classifies ACOS to the second group containing both *bona fide* 4CL proteins and 4CL-like ones that are apparently specific to land plants. All ACOS members are present in angiosperms and mosses only, and individual ACOS member has only a single copy in its genome. Different from most land plant-specific members in the group, sequences of ACOS proteins do not contain a consensus PTS1 (peroxisomal target sequence) at their C-termini, which can target the proteins to peroxisomes. Therefore, ACOS proteins are likely non-peroxisomal, and most closely related to true 4CL proteins (de Azevedo Souza et al. 2008). The true biochemical and developmental functions of ACOS were not clear until ACOS5 in Arabidopsis (de Azevedo Souza et al. 2009) and NtACOS1 in tobacco (Lin 2012; Wang et al. 2013) were investigated, which demonstrated that ACOS function is not like 4CL, instead it regulates the biosynthesis of lipid for pollen exine formation. Because similar enzymes are evolutionarily conserved in both angiosperms and Physcomitrella, ACOS represents a group of ancient and conserved enzymes in land plants. It is hypothesized that ACOS and 4CL proteins are recruited from lipid metabolism during early land plant evolution, to perform important functions in reproductive development, since dysfunction of ACOS enzymes often results in male sterility (Li et al. 2010; Chen et al. 2011; Shi et al. 2011; Yang et al. 2014). Expressions of all reported *ACOS* genes are preferentially in tapetal cells (Lin 2012; Bolaños-Villegas et al. 2013) or male flowers (de Azevedo Souza et al. 2008), which is well consistent with their functions in fertility.

In the present study, we confirmed that OsACOS12 is a cytoplasmic acyl CoA synthetase and an ancient land plant-specific enzyme with important functions in pollen development. Unlike its orthologous genes in dicots such as Arabidopsis and tobacco, OsACOS12 can play important roles in rice tapetum development and anther cuticle formation. Therefore, it has retained conserved ACOS functions among angiosperms while developed divergent functions during evolution. The phylogenetic analysis has revealed more ACOS orthologous genes presenting in other agronomic important crops including soybean, sorghum, and maize (Fig. 8), which highlights the need for comparative studies of more ACOS members among different species to fully understand their biochemical, physiological, and evolutionary functions in the future. Although in vivo activity of OsACOS12 has not been determined, in vitro enzyme activity assay clearly shows that OsACOS12 can take fatty acids with different carbon length or hydroxyl groups as substrates with CoA to make fatty acyl-CoAs that have multiple fates in the early upstream lipid metabolism for male fertility. It will also be interesting to investigate the biosynthesis of tetraketide α-pyrone in the future. Tetraketide α-pyrone is the downstream end product of ACOS enzymes and important structural components of pollen sporopollenin in Arabidopsis and tobacco. The level of tetraketide α-pyrone is significantly reduced in *NtACOS1 RNAi* mutant (Wang et al. 2013). Sequential enzymatic assays using NtACOS1-NtPKS1 or NtACOS1-NtPKS1-NtTKPR1 indicated that NtACOS1 takes fatty acids (in-chain and ω-hydroxyl) of various chain lengths to generate fatty acyl-CoAs for NtPKS1-mediated reactions, and the resulting products serve as substrates in the next reactions for NtTKPR1. This is similar to the metabolic pathway in Arabidopsis for the generation of reduced tetraketide α-pyrone (Grienenberger et al. 2010; Kim et al. 2010). Recombinant rice OsPKS1 and OsTKPR1 have also been reported to function downstream of NtACOS1. Thus, a metabolic pathway that starts from the formation of fatty acyl-CoAs by ACOS, continues with sequential condensations by PKS1/2, and ends with reduction by TKPR1/2 is likely conserved and indispensable for male reproduction in land plants.

Author contribution statement DZ, WL, and JS conceived and supervised the experiments; XY performed most of the experiments; JS, MC, and XZ provided technical assistance to XY; JS and XY analyzed the data and wrote the article with contributions of all authors, DZ and JS revised and finalized the manuscript. All authors read and approved the final version of the manuscript.

Accession numbers Sequence data from this article can be found in the EMBL/GenBank data libraries under following accession numbers: *OsACOS12* (Os04g0310700), *DPW* (Os03g0167600), *CYP704B2* (Os03g0168600), *CYP703A3* (Os08g0131100), *TDR* (Os02g0120500), *EAT1* (Os04g0599300), *OsAPI5* (Os02g0313400), *GAMYB* (Os01g0812000).

Acknowledgements We thank Lu Zhu (Shanghai Jiao Tong University, SJTU) for help in electron microscopy, Dr. Guorun Qu and Ms. Qian Luo (SJTU) for help in wax and cutin analysis. We appreciate very much to Dr. Sheng Quan (from the SJTU-Metabolon Joint Metabolomics Laboratory) for his critical reading and editing of the Manuscript. This work was supported by funds from the National Key Research and Development Program of China (2016YFD0101107); National Key Technologies Research and Development Program of China (2016YFD0100804); China Innovative Research Team, Ministry of Education, and the Programme of Introducing Talents of Discipline to Universities (111 Project, B14016); The Science and Technology Commission of Shanghai Municipality (13JC1408200).

Compliance with ethical standards

Conflict of interest The authors declare that there is no conflict of interest.

References

Ariizumi T, Toriyama K (2011) Genetic regulation of sporopollenin synthesis and pollen exine development. Ann Rev Plant Biol 62:437–460

Bolaños-Villegas P, Yang X, Wang HJ, Juan CT, Chuang MH, Makaroff CA, Jauh GY (2013) Arabidopsis CHROMOSOME TRANSMISSION FIDELITY 7 (AtCTF7/ECO1) is required for DNA repair, mitosis and meiosis. Plant J 75:927–940

Chen L, Chu H, Yuan Z, Pan A, Liang W, Huang H, Shen M, Zhang D, Chen L (2006) Isolation and genetic analysis for rice mutants treated with 60 Co γ-Ray. J Xiamen Univ 45:82–85

Chen W, Yu XH, Zhang K, Shi J, De Oliveira S, Schreiber L, Shanklin J, Zhang D (2011) Male Sterile2 encodes a plastid-localized fatty acyl carrier protein reductase required for pollen exine development in Arabidopsis. Plant Physiol 157:842–853

Choi H, Jin JY, Choi S, Hwang JU, Kim YY, Suh MC, Lee Y (2011) An ABCG/WBC-type ABC transporter is essential for transport of sporopollenin precursors for exine formation in developing pollen. Plant J 65:181–193

de Azevedo Souza C, Barbazuk B, Ralph S, Bohlmann J, Hamberger B, Douglas C (2008) Genome-wide analysis of a land plant-specific acyl:coenzyme A synthetase (ACS) gene family in Arabidopsis, poplar, rice and Physcomitrella. New Phytol 179:987–1003

de Azevedo Souza C, Kim SS, Koch S, Kienow L, Schneider K, McKim SM, Haughn GW, Kombrink E, Douglas CJ (2009) A novel fatty Acyl-CoA Synthetase is required for pollen development and sporopollenin biosynthesis in Arabidopsis. Plant Cell 21:507–525

Dobritsa AA, Shrestha J, Morant M, Dobritsa AA, Shrestha J, Morant M, Pinot F, Matsuno M, Swanson R, Møller LB, Preuss D (2009) CYP704B1 is a long-chain fatty acid omega-hydroxylase essential for sporopollenin synthesis in pollen of Arabidopsis. Plant Physiol 151:574–589

Fernández Gómez J, Talle B, Wilson Z (2015) Anther and pollen development: a conserved developmental pathway. J Integr Plant Biol 57(11):876–891

Goldberg RB, Beals TP, Sanders PM (1993) Anther development: basic principles and practical applications. Plant Cell 5:1217–1229

Gómez J, Talle B, Wilson Z (2015) Anther and pollen development: a conserved developmental pathway. J Integr Plant Biol 57:876–891

Grienenberger E, Kim SS, Lallemand B, Geoffroy P, Heintz D, de Azevedo Souza C, Heitz T, Douglas CJ, Legrand M (2010) Analysis of TETRAKETIDE alpha-PYRONE REDUCTASE function in *Arabidopsis thaliana* reveals a previously unknown, but conserved, biochemical pathway in sporopollenin monomer biosynthesis. Plant Cell 22:4067–4083

Ischebeck T (2016) Lipids in pollen—they are different. Biochem Biophys Acta 1861:1315–1328

Jiang J, Zhang Z, Cao J (2013) Pollen wall development: the associated enzymes and metabolic pathways. Plant Biol 15:249–263

Jung KH, Han MJ, Lee DY et al (2006) Wax-deficient anther1 is involved in cuticle and wax production in rice anther walls and is required for pollen development. Plant Cell 18:3015–3032

Kim SS, Grienenberger E, Lallemand B et al (2010) LAP6/POLYKETIDE SYNTHASE A and LAP5/POLYKETIDE SYNTHASE B encode hydroxyalkyl alpha-pyrone synthases required for pollen development and sporopollenin biosynthesis in *Arabidopsis thaliana*. Plant Cell 22:4045–4066

Lallemand B, Erhardt M, Heitz T, Legrand M (2013) Sporopollenin biosynthetic enzymes interact and constitute a metabolon localized to the endoplasmic reticulum of tapetum cells. Plant Physiol 162:616–625

Li H, Zhang D (2010) Biosynthesis of anther cuticle and pollen exine in rice. Plant Signal Behav 5:1121–1123

Li N, Zhang DS, Liu HS et al (2006) The rice tapetum degeneration retardation gene is required for tapetum degradation and anther development. Plant Cell 18:2999–3014

Li H, Pinot F, Sauveplane V et al (2010) Cytochrome P450 family member CYP704B2 catalyzes the {omega}-hydroxylation of fatty acids and is required for anther cutin biosynthesis and pollen exine formation in rice. Plant Cell 22:173–190

Li X, Gao X, Wei Y, Deng L, Ouyang Y, Chen G, Li X, Zhang Q, Wu C (2011) Rice APOPTOSIS INHIBITOR5 coupled with two DEAD-box adenosine 5′-triphosphate-dependent RNA helicases regulates tapetum degeneration. Plant Cell 23(4):1416–1434

Li Y, Li D, Guo Z, Shi Q, Xiong S, Zhang C, Zhu J, Yang Z (2016) OsACOS12, an orthologue of Arabidopsis acyl-CoA synthetase5, plays an important role in pollen exine formation and anther development in rice. BMC Plant Biol 16:256

Li-Beisson Y, Shorrosh B, Beisson F et al (2010) Acyl-lipid metabolism. Arabidopsis Book 11:e0161

Lin Y (2012) Functional analysis of anther-specific genes essential for pollen exine development and male fertility in tobacco. Ph. D thesis from The University of Hong Kong

Morant M, Jorgensen K, Schaller H, Pinot F, Moller BL, Werck-Reichhart D, Bak S (2007) CYP703 is an ancient cytochrome

P450 in land plants catalyzing in-chain hydroxylation of lauric acid to provide building blocks for sporopollenin synthesis in pollen. Plant Cell 19:1473–1487

Niu N, Liang W, Yang X, Jin W, Wilson ZA, Hu J, Zhang D (2013) EAT1 promotes tapetal cell death by regulating aspartic proteases during male reproductive development in rice. Nat Commun 4:1445

Parish R, Li S (2010) Death of a tapetum: a programme of developmental altruism. Plant Sci 178:73–89

Parish R, Phan H, Iacuone S, Li S (2012) Tapetal development and abiotic stress: a centre of vulnerability. Funct Plant Biol 39:553–559

Qin M, Tian T, Xia S, Wang Z, Song L, Yi B, Wen J, Shen J, Ma C, Fu T, Tu J (2016) Heterodimer formation of BnPKSA or BnPKSB with BnACOS5 constitutes a multienzyme complex in tapetal cells and is involved in male reproductive development in *Brassica napus*. Plant Cell Physiol 57:1643–1656

Schnurr J, Shockey J, Browse J (2004) The acyl-CoA synthetase encoded by LACS2 is essential for normal cuticle development in Arabidopsis. Plant Cell 16:629–642

Shi J, Tan H, Yu XH et al (2011) Defective pollen wall is required for anther and microspore development in rice and encodes a fatty acyl carrier protein reductase. Plant Cell 23:2225–2246

Shi J, Cui M, Yang L, Zhang D (2015) Genetic and biochemical mechanisms of pollen wall development. Trends Plant Sci 20:741–753

Shockey J, Browse J (2011) Genome-level and biochemical diversity of the acyl-activating enzyme superfamily in plants. Plant J 66:143–160

Tan H, Liang W, Hu J, Zhang D (2012) MTR1 encodes a secretory fasciclin glycoprotein required for male reproductive development in rice. Dev Cell 22:1127–1137

Varbanova M, Atanassov A, Atanassov I (2003) Anther-specific coumarate CoA ligase-like gene from Nicotiana sylvestris expressed during uninucleate microspore development. Plant Sci 164:525–530

Wallace S, Chater CC, Kamisugi Y, Cuming AC, Wellman CH, Beerling DJ, Fleming AJ (2015) Conservation of Male Sterility 2 function during spore and pollen wall development supports an evolutionarily early recruitment of a core component in the sporopollenin biosynthetic pathway. New Phytol 205:390–401

Wang Y, Lin YC, So J, Du Y, Lo C (2013) Conserved metabolic steps for sporopollenin precursor formation in tobacco and rice. Physiol Plant 149:13–24

Weber H (2002) Fatty acid-derived signals in plants. Trends Plant Sci 7:217–224

Weng H, Molina I, Shockey J, Browse J (2010) Organ fusion and defective cuticle function in a *lacs1lacs2* double mutant of Arabidopsis. Planta 231(5):1089–1100

Wilson ZA, Zhang DB (2009) From Arabidopsis to rice: pathways in pollen development. J Exp Bot 60:1479–1492

Xu J, Yang C, Yuan Z, Zhang D, Gondwe MY, Ding Z, Liang W, Zhang D, Wilson ZA (2010) The ABORTED MICROSPORES regulatory network is required for postmeiotic male reproductive development in *Arabidopsis thaliana*. Plant Cell 22:91–107

Xu J, Ding Z, Vizcay-Barrena G, Shi J, Liang W, Yuan Z, Werck-Reichhart D, Schreiber L, Wilson ZA, Zhang D (2014) ABORTED MICROSPORES acts as a master regulator of pollen wall formation in Arabidopsis. Plant Cell 26:1544–1556

Yang X, Wu D, Shi J et al (2014) Rice CYP703A3, a cytochrome P450 hydroxylase, is essential for development of anther cuticle and pollen exine. J Integr Plant Biol 56:979–994

Yuan X, Wei J, Zhang F, Zhou S, Zhang W (2011) Expression analysis of anACOS5 rice homologue in floret. J Shanghai Norm Univ (Nat Sci) 40:244–248

Zhang D, Wilson ZA (2009) Stamen specification and anther development in rice. Chin Sci Bull 54:2342–2353

Zhang H, Liang WQ, Yang XJ, Luo X, Jiang N, Ma H, Zhang DB (2010) Carbon Starved Anther encodes a MYB domain protein that regulates sugar partitioning required for rice pollen development. Plant Cell 22:672–689

Zhang D, Luo X, Zhu L (2011) Cytological analysis and genetic control of rice anther development. J Genet Genom 38:379–390

Zhang D, Shi J, Yang X (2016) Role of lipid metabolism in plant pollen exine development. In: Nakamura Y, Li-Beisson Y, eds. Lipids in plant and algae development. Springer, Geneva, pp 315–337

Zhao G, Shi J, Liang W, Xue F, Luo Q, Zhu L, Qu G, Chen M, Schreiber L, Zhang D (2015) Two ATP Binding Cassette G (ABCG) transporters, OsABCG26 and OsABCG15, collaboratively regulate rice male reproduction. Plant Physiol 169:2064–2079

Zhu L, Shi J, Zhao G, Zhang D, Liang W (2013) Post-meiotic deficient anther1 (PDA1) encodes an ABC transporter required for the development of anther cuticle and pollen exine in rice. J Plant Biol 56:59–68